Novel bio-conjugate materials: soybean peroxidase immobilized on bioactive glasses containing Au nanoparticles

UNIVERSITÀ DEGLI STUDI DI TORINO

Novel bio-conjugate materials: soybean peroxidase immobilized on bioactive glasses containing Au nanopaticles

V. Aina, T. Marchis, G. Cerrato, E. Laurenti, C. Morterra*

Dipartimento di Chimica IFM & Centro di Eccellenza Interdipartimentale "NIS", Università di Torino, Via P. Giuria 7, 10125 Torino, Italy; INSTM (Italian National Consortium for Materials Science and Technology), UdR Università di Torino.

L. Bergandi, D. Ghigo

Dipartimento di Genetica, Biologia e Biochimica, Università di Torino, Via Santena 5/bis, 10125 Torino, Italy.

G. Lusvardi, G. Malavasi, L. Menabue

Dipartimento di Chimica, Università di Modena e Reggio Emilia, Via Campi 183, 41125 Modena, Italy

* to whom correspondence should be addressed:

Prof. Claudio Morterra, E-mail address: claudio.morterra@unito.it

Tel +39-011-670-7589; Fax +39-011-670-7855.

Abstract

In the field of implantation, the delivery and/or immobilization of biomolecules developing a specific action on the bone mineralization process has attracted in the last years much attention. In fact, a wide spectrum of enzymes and proteins have been grafted with different methods onto/within implanted materials.

Bioactive glasses and glass–ceramics, due to their tailorable properties in terms of chemical composition, reactivity, and easiness of manufacturing, represent good substrates for enzymes immobilization. These biomaterials are well known for their peculiar surface reactivity promoting, when contacted with real or simulated body fluids, the formation of an hydroxo-apatite and/or hydroxy-carbonate apatite layer.

The aim of the present contribution is to immobilize, *via* a covalent linkage, an enzyme on the glass surface through the formation of self-assembled monolayers (SAMs), in order to obtain a stable bio-conjugate useful as a material bio-implantable into the human body.

The innovation of this study resides in the use of a new method of protein immobilization on the glass surface. Unlike other works, in which a preliminary silanization process has often been used, the introduction of gold nanoparticles (AuNPs) in the glass composition allowed us to exploit the easy SAMs formation process on the AuNPs dispersed in the bioactive glass matrix and, consequently, to immobilize an enzyme (soybean peroxidase, SBP, in the present case) on the SAMs. A thorough characterization of the materials, at different steps of the functionalization process, has been also reported, together with *in-vitro* activity tests of SBP and cytotoxicity tests using human osteoblast (MG-63) cells. The results obtained with immobilized SBP have been compared with those relative to merely adsorbed SBP.

Overall, a new bio-conjugate material, able to maintain its activity over time and to decrease the oxidative stress when in contact with MG-63 cells, has been obtained.

Key words: prosthesis implantation; enzyme immobilization; soybean peroxidase (SBP); bioactive glasses; oxidative stress; *in vitro* tests.

Introduction

Bone defects can be generated by a variety of events, like tumor resection, periodontal resorption, trauma, congenital defects, and arthroplasty revision surgery. [1] Improvements in bone implant integration and bone regeneration at surgical sites are still unresolved problems in orthopaedic and dental surgery. [2]

In recent years the research activity has been increasingly directed towards the specific preparation of defined biochemical surface properties on implantable biomaterials. [3-4]

New strategies to provide an appropriate environment for bone regeneration have been investigated. The delivery and/or immobilization of biomolecules with a specific action on the bone mineralization process has attracted much attention. [5-6] In fact, a wide spectrum of enzymes and proteins have been grafted onto or within implanted materials with different methods: *(i)* encapsulation, *(ii)* physical adsorption, *(iii)* covalent bonding. [5]

Sol-gel enzyme encapsulation has been one of the first and most popular immobilization techniques used so far, [7] because it can prevent the enzyme from unfolding and denaturation. However, encapsulation requires careful optimization processes to avoid leaching. Often, the encapsulation process causes a strong decrease of the enzyme activity because of the limitations in the substrates and products diffusion generated by the incorporation of the enzyme inside the carrier. On the other hand, physical adsorption [8] is the simplest method used to immobilize an enzyme onto the carrier surface, but the reversibility of this process and the prevalence of electrostatic and hydrophobic interactions do not allow a gradual release of biomolecules and can induce conformational changes of the native biomolecule structure. Finally, the use of protein coupling agents for the covalent immobilization allows to obtain stable and reproducible devices with controlled protein release and with limited effects on the structure and properties of the enzyme. [9] In this context, bioactive glasses and glass–ceramics, due to their tailorable properties in terms of chemical composition, reactivity, and easiness of manufacturing, [10] represent a good substrate for enzymes immobilization. These materials are well known for their peculiar surface reactivity: when they are

in contact with water or aqueous solutions, as simulated body fluids (SBF), [11] bioactive glasses stimulate in vivo the precipitation of a layer of hydroxy-carbonate apatite (HCA) on their surfaces, promoting the implant osteointegration. [12]

The most common approach for the covalent bonding of biomolecules on glasses surface, used since the pioneering studies of Weetall *et al*. [13-14], is the silanization of the ceramic surface with a sol–gel precursor, followed by the attachment of a protein coupling agent, such as glutaraldehyde. [15]

Recently, the self-assembly (SA) technique has been widely investigated for the bio-conjugation of a wide variety of solid surfaces, especially via the formation of self-assembled monolayers (SAMs). [16] SAMs are monomolecular films of surfactants that spontaneously adsorb/chemisorb onto solid surfaces (for instance, metals such as gold, silver, copper, titanium, etc., and oxides such as silica). The wide range of surfactants that can be used to form such monomolecular systems provides a method to functionalize biomaterials that is convenient, versatile, flexible, and simple. In the biomedical field, nano-sized supports are receiving growing interest for protein and drug delivery applications. [17] Au nanoparticles (AuNPs) have been recently reviewed as highly promising drug delivery systems (DDS). [18-19] The ease of functionalization of AuNPs makes them a versatile tool in delivery method, with unique chemical and physical properties. Moreover, gold core has been demonstrated to be essentially non-toxic and biocompatible, and this makes it an ideal starting point for carriers construction. [19] To this purpose, sol-gel bioactive glasses containing AuNPs have been synthesized and completely characterized in a previous contribution. [20]

The sol-gel synthesis methodology yields high surface area materials whereas the glasses descending from Bioglass 45S5 discovered by Hench in the 1970s, possess a very low surface area. Sol-gel bioactive glasses represent a second generation of bioactive materials thanks to their high surface area, interact fast and efficiently with the biological fluids, and allow a rapid growth of HCA**.;** Their composition can deviate dramatically from the Bioglass-45S5 composition, in that *sol-gel* glasses are typically sodium-free and can be very rich in silica (up to 80% weight SiO_2).

The present research work is devoted to immobilize, via a covalent linkage, an enzyme onto the glass surface through the formation of SAMs on AuNPs dispersed in the bioactive glass, in order to obtain stable bio-conjugates useful as materials bio-implantable into the human body.

The so-called surgical stress response is a well defined physiological mechanism that involves, during and after surgical procedures, the activation of inflammatory, endocrine, metabolic and immunologic mediators. [21-22]

Surgical stress also includes the occurrence of oxidative stress, with production of reactive oxygen (ROS) or nitrogen species (RNS) that may overwhelm the defence systems of the organism. It has been demonstrated that the administration of antioxidants results in improved organ function, shortened convalescence, reduced morbidity and mortality occurring in the surgical stress response. [22] The antioxidant defence mechanisms are numerous, and include enzymatic as well as non enzymatic mechanisms. Some of the most important antioxidant enzymes are superoxide dismutase (SOD), catalase and peroxidases: SOD is able to convert superoxide anions to the less toxic hydrogen peroxide, thus reducing the formation of the highly reactive peroxynitrite ($ONOO^-$), whereas catalase and peroxidases metabolize H_2O_2. [21,23]

Mammalian peroxidases appear to play a role in extracellular defence against pathogens and stress by oxidising chloride, bromide or thiocyanate to form hypohalides or hypopseudohalides (*i.e.* hypochlorous acid, hypothiocyanate, etc.) that have strong bactericidal or bacteriostatic action, but their reactivity, is non specific and can attack both pathogen and host tissue. [22,24,25] On the contrary, plant peroxidases are quite different. In particular, peroxidases belonging to the extracellular Class III superfamily have a slightly lower oxidant potential, but are suitable for detoxification and scavenging of ROS and RNS. [26-27] Soybean peroxidase (SBP) possesses high stability toward thermal and chemical denaturation that renders it particularly appropriate for covalent immobilization. [28-31]

For these reasons, in the present study SBP has been chosen for immobilization on bioactive glasses, with the aim of improving the glass bioactivity and decreasing the oxidative stress phenomena as a consequence of material implantation.

To the best of our knowledge, this is the first time that SAMs formation has been exploited to obtain an enzyme-support bio-conjugate onto sol-gel bioactive glasses. We will herewith demonstrate that this type of technique is easy to use, and allows to obtain stable and reproducible devices.

The innovative aspect of the present contribution resides in the use of a new method for proteins immobilization on a glass surface. In fact, unlike other works in which the conventional silanization process has been used, [32-33] the introduction of AuNPs in the glass composition should allow to exploit the easy process of SAMs formation on AuNPs and, consequently, to immobilize SBP on the SAMs. Moreover, a thorough characterization of the functionalized material, isolated at different steps of the process, will be reported, together with *in-vitro* activity tests of SBP as well as cytotoxicity tests using osteoblast (MG-63) cells. The results of immobilized SBP will be compared with those of merely adsorbed SBP.

Materials

2.1 Glasses synthesis

As reported in detail elsewhere, [20] two glass systems with molar composition $15CaO{\cdot}5P_2O_5{\cdot}80SiO_2{\cdot}xAu_2O$ (with x = 0 and 1; the gold amount is indicated in the conventional oxidic form Au_2O) were synthesized, using a sol-gel route. The glasses powders were ground in an agate mortar and sieved, in order to isolate the fraction of particles with Ø < 50μm.

The glasses are in the following referred to as SG (x = 0) and SGAu (x = 1), respectively.

2.2 Enzyme immobilization

The covalent immobilization of SBP onto SGAu was obtained (see **Scheme 1**) through the sequence: (a) the coating of AuNPs with cysteamine, obtained by selective via-thiol chemisorption, and leading to the functionalization of the surface with external reactive amino groups; (b) and (c) the successive double conjugation reaction achieved by the *bis*-aldehyde homobifunctional linker, glutaraldehyde, between the external amino groups available onto cysteamine-modified AuNPs and SBP, respectively.

(a) The AuNPs surface was functionalized with cysteamine by dipping 400 mg of SGAu into 25 ml of ethanol solution of cysteamine 10 mM under Ar flow in order to remove air traces. After stirring for 24 hours at 4°C in a vessel protected from light, the suspension was filtered, washed with ethanol and bidistilled water, and dried under gentle nitrogen gas flux.

(b) 300 mg of cysteamine-modified SGAu (SGAu-C) were added to 10 ml of glutaraldehyde water solution ($5.8{\cdot}10^{-2}$ M, phosphate buffer 50 mM pH 7.5, PBS) under Ar flow and stirred for 3 hours at RT, protected from light.

(c) The glutaraldehyde conjugated SGAu-C-G was washed many times with PBS and re-suspended into 5 ml of SBP solution 1 mg/ml (phosphate buffer 50 mM pH 7.5). The reaction vessel was kept at 4°C under stirring for 24 hours, protected from light.

(d) Hence, the solid phase was filtered and washed many times with the buffer solution. The samples of immobilized SBP (SGAu-C-G-SBP) were stored dry at 3°C.

The plain impregnation/adsorption of SBP onto the glass surface was achieved by directly dropping 300 mg of SGAu glass into 5 ml of SBP solution 1 mg/ml. The glass sample was then filtered, washed, dried, and stored at 3°C (SGAu-SBP-Ads).

The amount of enzyme loaded onto SGAu-C-G-SBP was calculated as the difference between the enzyme amount in the initial solution (solution 1 mg of SBP per ml of phosphate buffer) and the enzyme amount in the filtrate (protein solution after contact with glass and after washing). The quantification of the SBP in solution was determined spectroscopically by means of the absorbance of Soret band at 403 nm with extinction coefficient ε_{403nm} = 94600 $M^{-1}cm^{-1}$. [34] All UV-Vis measurements were acquired with a UNICAM UV300 Thermospectronic double beam spectrometer, equipped with a Peltier cell for temperature control.

Methods

2.3 Glasses characterization

IR spectroscopy. Conventional IR KBr pellets were prepared by mixing the functionalized glass samples and KBr at a 1 : 20 ratio. All transmission FTIR spectra of KBr pellets were obtained, in the 4000–400 cm^{-1} spectral range, with a Bruker IFS 28 spectrometer, using a DTGS detector in order to inspect the low-υ region down to 400 cm^{-1}, and accumulating for each measurement 128 scans at 4 cm^{-1} resolution.

Elemental analysis. The amount of cysteamine, glutaraldehyde and SBP loaded on the glass was estimated by the evaluation of the percent content of N, C, H and S (Elemental Analysis CE Instrument, mod. EA1 110).

Scanning electron microscopy (SEM). The modifications of gel glass surface morphology after the different functionalization steps and after *in vitro* bioactivity tests were evaluated by means of environmental scanning electron microscopy (ESEM; FEI Quanta 200, Fei Company, The Netherlands), equipped with an energy dispersive spectroscopy (EDS) instrument (INCA 350, Oxford Instruments, UK).

X-Ray diffraction (XRD). The evolution of crystal phase after bioactivity tests was studied by means of a diffractometer (Panalytical X'PertPro, The Netherlands) equipped with Ni-filtered Cu Kα radiation, λ = 1.54060 Å, in the 2θ range 10-50° with time step 50 s and scan size 0.03°.

2.4 Glasses functionalization stability and in vitro bioactivity.

The stability of the bond formed between the ligands and/or protein and AuNPs was investigated by dipping a sample of functionalized SGAu (250 mg) in 15 ml of cells culture medium (MEM, Minimum Essential Medium Eagle with Earl's salts), and monitoring the release of the ligand after 1 hour, 1 day and 7 days. The release and bioactivity studies were performed by the use of: *(i)* FTIR spectroscopy, *(ii)* XRD, and *(iii)* SEM analysis on the glasses deriving from filtered and washed aliquots of the initial suspension.

2.5 Enzyme activity

The catalytic activity of SBP was measured using 3-methyl-2-benzothiazolinone hydrazone (MBTH) and 3-(dimethylamino)benzoic acid (DMAB) as substrates. In the presence of H_2O_2, the enzyme catalyses the oxidative dehydrogenation of MBTH, which in turn reacts with DMAB to give a purple product easily detectable by UV-vis spectroscopy. [35]

(i) The activity essay was carried out by varying the enzyme concentration between $1.25 \cdot 10^{-9}$ M and $2.00 \cdot 10^{-8}$ M with $1.20 \cdot 10^{-3}$ M DMAB, $3.73 \cdot 10^{-5}$ M MBTH and $4.9 \cdot 10^{-5}$ M H_2O_2. The initial reaction rates were detected at wavelength λ_{max} = 590 nm, with extinction coefficient ε_{590} = 47600 M^{-1} cm^{-1}.

In the case of immobilized samples, the appropriate concentration of enzyme was obtained preparing an initial suspension of 10 mg/ml of SGAu-C-G-SBP, left under stirring for 1 hour before measurements, from which an appropriate aliquot was withdrawn and added to the reaction vessel. The volume of each aliquot volume was calculated on the basis of the estimated enzyme load.

(ii) With the same DMAB/MBTH assay, a discontinuous dosage test was also performed: the absorbance of the coloured product was measured after 10 minutes of reaction catalysed by SGAu as synthesized, SGAu-C, SGAu-C-G, immobilized SBP (SGAu-C-G-SBP), and adsorbed SBP (SGAu-SBP-Ads), at equal concentrations of solid suspensions (1.6 mg SGAu/ml). A further test

has been carried out also on free SBP in solution at the same molar concentration of the immobilized sample.

2.6 Cytotoxicity tests

Cells and reagents

MG-63 human osteoblast cells (provided by Istituto Zooprofilattico Sperimentale "B. Ubertini", Brescia, Italy) were cultured up to confluence in 35-150 mm diameter Petri dishes with MEM supplemented with 2% foetal bovine serum (FBS), penicillin, streptomycin and L-glutamine in a humidified atmosphere containing 5% CO_2 at 37°C. Before the assays, the confluent cells were incubated for 24 hours in the absence or presence of glasses and other reagents, as described in the following paragraphs.

The protein contents of cell monolayers and cell lysates were assessed with the BCA kit from Pierce (Rockford, IL). Plastic-ware was from Falcon (Becton Dickinson, Franklin Lakes, NJ). Unless otherwise specified, other reagents were purchased from Sigma Aldrich (Milan, Italy).

Lactate dehydrogenase (LDH) leakage. To check the cytotoxic effect of the different experimental conditions described in the *Results* section, LDH activity was measured on aliquots of culture supernatant and in the cell lysate at the end of the 24 hours incubation time in the absence or presence of glasses and other reagents, as also described previously. [36] Both intracellular and extracellular enzyme activities, measured spectrophotometrically as absorbance variation at 340 nm (37°C), were expressed as μmol of reduced nicotinamide adenine dinucleotide (NADH) oxidized/min/dish, then extracellular LDH activity was calculated as a percentage of the total (intracellular + extracellular) LDH activity in the dish.

Measurement of malonyldialdehyde (MDA). After 24 hours incubation with bioactive glasses and/or other substances, cells were washed with PBS, detached with trypsin/EDTA, and re-suspended in 1 ml of PBS. The lipid peroxidation was spectrophotometrically detected with a Packard EL340 microplate reader (Bio-Tek Instruments, Winooski, VT) measuring the intracellular level of MDA, the end product derived from the breakdown of polyunsaturated fatty acids and related esters, with

the lipid peroxidation assay kit (Oxford Biomedical Research, Oxford, MI), which uses the reaction of N-methyl-2-phenylindole with MDA in the presence of hydrochloric acid to yield a stable chromophore with maximal absorbance at 586 nm. [37] Intracellular MDA was expressed as pmol/mg cellular protein.

Statistical analysis. All data in text and figures are provided as means ± SE. The results were analyzed by a one-way analysis of variance and Tukey's test. $P < 0.05$ was considered significant.

Results and Discussion

3.1 Glass functionalization and protein immobilization

In this work, the presence of AuNPs dispersed on the glass surface (see the white particles in the inset image of **Figure 1, section A** and, for a thorough characterization, the work by Lusvardi *et al*. [20]) gives us the possibility to exploit the formation of SAMs on the gold surface, and to immobilize thereon the SBP enzyme. For simplicity, in the following we will refer to the samples of interest using the abbreviations reported in **Table 1**.

Scheme 1 is representative of the three steps involved in the process of SBP covalent immobilization: the first step is the coating of AuNPs with cysteamine ***(step a)***, the second step is the conjugation of glutaraldehyde ***(step b)*** and, finally, the third step is the attachment of SBP ***(step c)***.

Each step of the functionalization/immobilization process was systematically characterized using SEM microscopy, FT-IR spectroscopy, XRD, and elemental analysis.

- In the first step ***(step a)***, in which the functionalization with cysteamine of AuNPs loaded on the bioactive glass was attempted, we expected, after contact with cysteamine solution at 4°C, a selective via-thiol chemisorption [38] leading to a glass functionalization with external reactive amino groups exposed at the surface. By inspection of FT-IR spectra and of elemental analysis data obtained after this first functionalization step, the presence of cysteamine on AuNPs dispersed on/in the glass matrix could be confirmed, as reported below.

In **sections A and B** of **Figure 1**, the (SEM-EDS) morphological evolution produced after the functionalization with cysteamine is reported. Actually, SEM analysis shows that, during the first functionalization step, only a slight modification of surface morphology occurred in that, after contact with cysteamine, the glass grain edges became a bit smoother. Also the semi-quantitative EDS analysis does not evidence a significant modification of the surface chemical composition.

Section A of **Figure 2** reports the KBr IR spectra of the Au-loaded glass as-such [spectrum (a)] and after functionalization with cysteamine [spectrum (b)]. For comparison purposes, also the spectrum

of pure cysteamine is presented [spectrum (1)]. It can be observed that, after contact, the whole complex vibrational envelope of cysteamine is clearly detectable in spectrum (b) of the functionalized glass. In particular, the following features can be singled out: *(i)* a band centred at 1587 cm^{-1}, ascribable to the $–NH_2$ deformation mode, [39] that would confirm that, after the first functionalization step, free amino functionalities are present at the glass surface; *(ii)* two bands of odd intensity at 1495 and 1325 cm^{-1}, ascribable to coupled $–CH_2$ deformation modes; *(iii)* a band at 1247 cm^{-1}, characteristic of the $–CH_2$-S wagging mode. [39] Overall, these spectral features indicate that the first functionalization step proceeded successfully.

The presence of linked cysteamine on SGAu-C samples is also attested by elemental analysis (see **Table 2**), that allowed us to determine 13.8 mg of cysteamine per gram of glass.

Figure 3 reports the XRD patterns of all studied samples. **Sections A and B** of the XRD analysis show only sharp reflections attributed to Au crystals (JCPDS 04-0784), [40] and a broad bump ($2\theta \approx 20\text{-}25°$) due to the amorphous silica-based glassy phase, [41] already present in the starting SGAu sample. In agreement with SEM-EDS results, this datum confirms that, in this first reaction step, no appreciable morphological/structural changes did occur.

- In the second step ***(step b)*** of the functionalization process, glutaraldehyde was introduced and was expected to react with free amino groups (see **Scheme 1**) of the SGAu-C glass, forming Schiff bases.

Section C of **Figure 1** indicates that, also in this reaction step, the (surface) morphology of the glass particles changed slightly, whereas the grains surface became covered by rod-like crystals not homogeneously distributed (see XRD section C of Figure D) made up of brushite.

The IR spectra of **Figure 2**, **Section B** evidence that the conjugation process has indeed occurred. In fact, spectrum (c), relative to the SGAu-C-G sample, clearly shows the presence of a band doublet at ~1672 cm^{-1}, ascribable to the carbonyl stretching vibration of aliphatic aldehydes. Little else could be said, from spectrum (c), on the "over-crowded" 1680-1200 cm^{-1} interval, but the differential segment termed (c)-(b) indicates that, in this reaction step, a complex spectral envelope

closely corresponding to glutaraldehyde [compare (c)-(b) with spectrum (2)] was introduced in the overall 1680-1200 cm^{-1} spectrum. It is somewhat surprising that the differential segment (c)-(b) does not show clear evidence for the consumption of the $–NH_2$ band at ~1590 cm^{-1} (it should appear in (c)-(b) as a negative or downward contribution to the overall differential bands envelope), and this suggests that only a relatively small fraction of the surface $–NH_2$ functionalities did react with the aldehyde.

Also in this case, elemental analysis was carried out on the reacted system, and the presence of glutaraldehyde after conjugation was confirmed by the percent increment of C with respect to the first functionalization step (see **Table 2**). Compared to the amount of linked cysteamine previously evaluated, the amount of glutaraldehyde corresponding to the observed increment of C is approximately only one half, in agreement with what already suggested by IR spectral data. This is probably because some of the abundant amino groups of linked cysteamine are inaccessible for the reaction with glutaraldehyde, due to steric hindrance.

The XRD pattern in **section C** of **Figure 3** reveals, besides Au, the presence of brushite crystals ($CaHPO_4 \cdot 2H_2O$; JCPDS 09-0077). Note that the typical PO stretching bands analytical of brushite (1135, 1081, 989 cm^{-1}) [39,42] cannot be singled out in the IR spectrum (c) of **Figure 2B**, as they lay “on top of” the strong (though not saturating) absorbance signal due to the O-Si-O stretching envelope of the silica network, where also intrinsically strong vibrational modes are either not visible or appear as weak as background noise (as it is the case also for some sharp 1200-1000 cm^{-1} features belonging to glutaraldehyde).

- The last step ***(step c)*** of the functionalization process is the immobilization of SBP on the SGAu-C-G sample.

From the inspection of **section D** of **Figure 1** it is clearly evident that this reaction step deeply modifies the sample morphology, as the surface of the large starting particles becomes homogeneously covered by small rod-like particles (length 2-10 μm). The Ca/P ratio determined by

EDS analysis changes significantly from 1.50 in the starting SGAu glass to 1.05 in the SGAu-C-G-SBP system. The latter ratio is fairly similar to that found in the brushite phase (Ca/P = 1.00).

Panel C of **Figure 2** reports the IR spectra of: the SGAu-C-G sample [spectrum (c)], SBP immobilized thereon [spectrum (d)], SBP adsorbed by impregnation on the non-functionalized SGAu glass [spectrum (e)], and pure SBP [spectrum (3), inserted for comparison]. In the fingerprint region, the spectrum of pure SBP is characterized by two bands of odd intensity, typical of proteins polypeptide chain, and usually called Amide I and II, centred at 1667 cm^{-1} (and ascribable to the (C=O) stretching mode of the carbonyl group), and at 1532 cm^{-1} (due to a combination of N-H and C-N stretching vibrations), respectively. Spectrum (d) and, better than that, the differential spectral segment termed (d)-(c) (bold line) clearly indicate the presence of two bands, very similar in position, shape, and relative intensity to those of the free enzyme and of the enzyme merely adsorbed/absorbed on SGAu. The presence of SBP on the surface of the functionalized glass is thus confirmed.

By the use of Elemental Analysis it was not possible to gain any reliable information about this last functionalization step, probably as a consequence of the relatively low amount of immobilized SBP.

The XRD pattern of **Figure 3**, **section D** (black line) shows with high intensity the peaks typical of the brushite phase. For instance, in the SGAu-C-G-SBP sample, the intensity of the analytical peak at $2\theta = 11.80°$ (d=7.52Å, I/I_0=100%) is 11360 counts, one order of magnitude higher with respect to that of the SGAu-C-G sample (compare with the black trace in **Figure 3C**). The formation of brushite can be attributed to the buffer (PBS) used in the second and third functionalization steps. Ca ions, released in solution by the glass dissolution process, [20] rapidly cause the precipitation of a Ca-phosphate phase and, in these conditions of high percent content of P, brought about by the buffer, the formation of a phase with a low Ca/P ratio is favoured. Brushite is indeed a crystalline Ca-phosphate phase with a low Ca/P ratio (1.00), whereas the Ca-phosphate phases commonly formed on bioactive glasses soaked in aqueous solutions are tri-calcium phosphate β-$Ca_3(PO_4)_2$ (β-TCP Ca/P=1.50) and, above all, hydroxy-apatite $Ca_5(PO_4)_3OH$ (HA; Ca/P=1.67). Brushite is a

precursor for the formation of TCP and/or HA, that are commonly regarded as the bioactive phases, [43-44] and for this reason the abundant presence of brushite on SGAu-C-G-SBP can be considered a favourable condition for the development of bioctivity. [43-44]

3.2 Glasses functionalization stability, and in-vitro bioactivity

In order to evaluate the degradation performance of functionalized materials, and the growth behaviour of HA (and, possibly, hydroxy-carbonate-apatite, HCA) as a function of soaking time in MEM solution, specific XRD, FT-IR, and SEM-EDS analyses were carried out.

Figure 4 presents the FT-IR spectra of AuNPs-glasses, either as-such (**Section A**) or after each step of the functionalization process (**Sections B-D**), isolated after 1 hour, 1 day, and 7 days reaction in MEM solution.

In the case of the non-functionalized starting glass SGAu (**Figure 4**, **Section A**), the comparison between spectra (d) and (a) indicates that, due to the appearance of a well resolved bands doublet at 611 and 560 cm^{-1}, crystalline phosphate of the HA/HCA type has grown on the glass surface in 7 days of reaction in MEM. [20] The powder XRD analysis of **Figure 3**, **Section A** reveals peaks at °2θ values around 26° and 32° that, by matching JCPDS files, are identified as the (002) and (211) reflections of HA, respectively (JCPDS 09-0432). [40] In addition to HA peaks, also a peak centered at °2θ ≈ 21° (d = 4.16 Å) and characteristic of SiO_2 gel [41]was identified. Also SEM analysis shows a significant modification of glass morphology after 7 days of soaking in MEM (see **Figure 5**, **section A**): after 7 days in MEM (for comparison purpose see **Figure 1, section A**), the glass surface turns out to be covered by aggregates with roundish contours essentially constituted by Ca, P and O with a Ca/P ratio = 1.61, fairly similar to that found in HA (Ca/P=1.67). From all these data is clearly evident that the SGAu material can be considered as bioactive.

In the case of the functionalized glass, FT-IR spectra of the systems SGAu-C (**Figure 4**, **Section B**), SGAu-C-G (**Figure 4**, **Section C**), and SGAu-C-G-SBP (**Figure 4**, **Section D**) show that: *(i)* the formation of crystalline apatite-like species on the glass surface is, in general terms, delayed. In fact, after 7 days of reaction in MEM [spectra (d)], in the case of the samples SGAu-C and SGAu-

C-G the presence of an amorphous Ca-phosphate species is still evident (broad and un-resolved band at ~565 cm^{-1}), whereas in the case of SGAu-C-G-SBP, after 7 days reaction, two bands of very low intensity, typical of crystalline HA formation, appear at 611 and 560 cm^{-1}; *(ii)* the spectral behaviour of the linked organic molecules (*i.e.*, cysteamine, glutaraldehyde, and peroxidase), evaluated by glass dissolution in MEM, evidences that, after up to 7 days of treatment, all of the organic components successively introduced are still abundantly present on the glass surface, even if the spectra in **Section C** and, even more, **Section D** suggest that a partial detachment of the organic functionality has occurred.

XRD (**Figure 3**, **Sections B, C,** and **D**) and EDS-SEM data (**Figure 5**, **Sections B, C,** and **D**) seem to confirm what suggested by the spectroscopic behaviour: *(i)* after 7 days of reaction in MEM, the SGAu-C sample still presents the same morphology, the same surface composition, and the same crystalline phases exhibited before soaking in MEM; *(ii)* in the case of the SGAu-C-G sample, MEM soaking caused, with contact time, an increase of the surface amount of brushite crystals (not detectable from IR spectra for the reasons already explained above); *(iii)* after 7 days of reaction of the SGAu-C-G-SBP sample, the amount of brushite phase seems to be far lower with respect to that detected on the sample before soaking (decrease/disappearance of XRD reflections typical of the brushite phase), while both XRD and EDS analyses (**Figures 1**, **section D**, and **5**, **section D**) seem to suggest the conversion of brushite into HA (broad XRD peak at $°2\theta \approx 32°$, and Ca/P ratio varied from 1.05 before soaking to 1.53 after MEM soaking).

Summarizing, it is possible to conclude that the functionalization steps with cysteamine and cysteamine + glutaraldehyde inhibit the formation of bioactive HA-like phases, whereas the presence of immobilized SBP favours the conversion of brushite (formed during the complex functionalization process) in a crystalline HA-like phase, monitoring bioactivity.

3.3 Enzyme loading and activity

The amount of SBP loaded on the bioactive glass was evaluated indirectly, using UV-Vis spectroscopy, from the difference between the enzyme content in the reaction supernatant and

washings. It has been so possible to calculate the enzyme loading on the solid carrier, both in the case of the immobilization and impregnation/adsorption procedures.

As expected, SBP immobilization was influenced by the initial concentration of SBP. In our experimental conditions, the best result was a loading of 1.38 mg SBP/g SGAu-C-G, with a percentage of immobilized enzyme at 10%, but corresponding to 50% of conjugation yield, as calculated on the basis of available aldehyde groups determined through elemental analysis.

However, protein loading is not the only parameter that characterizes an immobilized enzyme. Both the covalent bonding and the adsorption technique could have undesirable consequences on the enzymatic activity, in that: - the enzyme covalent binding on the support often leads to little leakage of catalytic activity, induced by the attachment of the enzyme in a non-productive conformation that can be related to limited accessibility and/or partial distortion of the catalytic site; - the case of enzymes adsorption on metallic NPs is driven by electrostatic interactions, that can lead to unfolding and inactivation. For this reason, the initial reaction rate by the DMAB/MBTH/H_2O_2 system has been measured, at increasing enzyme concentrations, for free SBP and for the SGAu-C-G-SBP and SGAu-SBP-Ads samples. The results, in terms of initial average rate of the oxidation product as a function of enzyme molar concentration, are reported in **Figure 6**. It is noted that, in all cases, the enzyme activity is proportional to the enzyme concentration, even if appreciable are the differences in slope. The increasing enzymatic activity as a function of enzyme concentration confirms that this immobilization technique minimized diffusion-limiting processes. As for the large difference (decrease) of maximum activity observed between free SBP in solution and immobilized SBP samples, it is thought to be ascribable to a partial loss of catalytic activity affecting the enzyme, after the covalent/adsorption immobilization.

Retained activities after the two immobilization processes (covalent and adsorption) were calculated as the ratio between the slopes of the regression equations obtained for the immobilized samples and free enzyme. As evident from **Figure 6**, the covalent immobilization (SGAu-C-G-SBP) shows a definitely higher activity yield (of 21.55%) with respect to the adsorbed sample (SGAu-SBP-Ads;

0.82%). The partial loss of activity exhibited by SGAu-C-G-SBP is comparable to that observed for SBP immobilized on aminopropyl glass beads (work in progress). As for the drastic decrease in activity yield observed for SBP adsorbed onto SGAu, it can be correlated with the direct interaction of the enzyme with the metallic surface.

In order to exclude a potential oxidative activity of the support, a comparison between relative activities of all the intermediate samples, representing the various steps of the immobilization process, was performed with a discontinuous test (absorbance of the oxidised product, measured at 590 nm, obtained after 10 minutes of reaction time), at constant solid suspension concentration (1.6 mg SGAu/ml). The results obtained were then related to the value acquired with free SBP in solution, using the same enzymatic concentration of SGAu-C-G-SBP. The results are listed in **Figure 7** in terms of percentage activity, having taken as 100% the activity of free SBP. The data reveal a little oxidative activity for SGAu as-such and for the first functionalized glass specimens, that goes from 5.2% for SGAu as-such to 17.2% for SGAu-C and 14.8% for SGAu-C-G. The values reported for the functionalized bioactive glasses reveal that the solid support explicates a little catalytic activity towards the DMAB/MBTH/H_2O_2 system. On the other hand, SGAu-C-G-SBP and adsorbed SBP percentages confirm that most of the contribution is substantially ascribable to the enzymatic action, that differs depending on the type of immobilization technique used. These data are in good agreement with specific activity results presented above (work in progress), and indicate that (especially for the 111.44% of SGAu-C-G-SBP) the support-contribution, although minimal, is cumulative to the enzymatic one.

3.4 Cytotoxicity tests

To check a possible cytotoxicity of the materials in the different steps of glass functionalization, LDH release and MDA production after 24 hours of glasses incubation with MG-63 cells have been evaluated.

The release of LDH in the extracellular medium is a sensitive index of cytotoxicity. [36] It is worth noting that, after 24 hours incubation, the AuNPs-containing glass as-such (SGAu) caused a

significant increase of LDH leakage at 50 and 100 μg/ml (corresponding to 12.5 μg/cm^2 and 25 μg/cm^2, respectively), but not at 25 μg/ml (6.25 μg/cm^2) (**Figure 8**). An increase of LDH release was also significant after a 24 hours incubation of the cells with 50 and 100 μg/ml of SGAu-C-G sample, and with the only glutaraldehyde at the concentrations of 5 and 10 nM that correspond to the amount of glutaraldehyde immobilized onto 50 and 100 μg/ml of glass, respectively. The cytotoxic effect caused by the glass SGAu as-such is probably due to the presence, already postulated elsewhere, [20] of some residual Au^{n+} species on the glass surface. When in contact with the cells, these species would tend to reduce to Au^0, causing an oxidative stress. In the case of SGAu-C-G, the free aldehydic termination is likely to be responsible for the cell damage, as confirmed by the similar cytotoxic behaviour of free glutaraldehyde. Glutaraldehyde is a commonly used crosslinking agent, for example in drug delivery matrices. Its toxicity has been shown to be concentration-dependent. [45] Glutaraldehyde can bind to DNA and proteins to form crosslinks through the N-terminal groups of nucleotides or amino acids to form molecular adducts. Previous studies have found that it is possible to decrease the cytotoxic effects of glutaraldehyde towards N-terminal groups of proteins and nucleotides by washing the materials with a phosphate buffer solution before the contact with cells or by using $_L$-glutamic acid and/or glycine to quench the aldehydic groups. [46-48]

In the case of SBP chemically immobilized or adsorbed on the glass surface, the cytotoxic effect of SGAu on the cells was completely abolished. A similar decrease was also detectable in the presence of only SBP. In the case of adsorbed SBP, it should be noted that the amount of protein adsorbed on the glass (with respect to the amount of immobilized protein) was lower, and that the activity of adsorbed protein (see SBP activity data, **Figure 6** and **Figure 7**) was reduced, probably due to the conformational changes of the native SBP structure.

A possible time-dependence of glass cytoxicity has been also evaluated, by incubating the materials of interest, at 50 μg/ml, for 3, 6, 24 and 48 hours. At 3 and 6 hours no effect has been detected,

whereas at 48 hours an effect at all similar to that found at 24 hours has been measured (data not shown for the sake of brevity).

On the basis of these LDH results, the production of MDA, a main product of the peroxidation of cells membrane lipids, has been evaluated after 24 hours of glasses incubation at the same concentrations. Also in this case the oxidative stress was detectable only after incubation with the same concentrations of SGAu, SGAu functionalized with both cysteamine and glutaraldehyde (SGAu-C-G), and with only glutaraldehyde (**Figure 9**) which produced an increase of LDH leakage.

Cytotoxicity data suggested that SBP immobilization on AuNPs bioactive glasses causes a significant reduction of the material cytotoxicity (cell damage and oxidative stress) in contact with osteoblast cells.

In order to evaluate the response of these materials after the so-called surgical stress involving the activation of inflammatory, endocrine, metabolic and immunologic mediators, in vivo tests will be performed. The in vivo response will be evaluate using female Swiss alpine sheep models.

A decrease of oxidative stress after the implantation of SBP functionalized AuNPs bioactive glasses with respect to AuNPs glass will be expected.

Conclusions

In this work a new method–of covalent enzyme immobilization onto sol-gel bioactive glasses surface has been proposed. This approach allows us to obtain stable and reproducible devices to be used as implanted biomaterials. In particular, this new bio-conjugate material was shown to be able to maintain its bioactivity over time, and to decrease the cell damage and oxidative stress.

The presence of AuNPs on the material surface turned out to be of vital importance for the immobilization/functionalization steps, as well as for the stability of the enzyme (SBP). In fact, after 7 days of treatment in solution, all of the organic components introduced during the functionalization steps (cysteamine, glutaraldehyde and, eventually, SBP) are still abundantly present on the glass surface.

The covalent immobilization process (SGAu-C-G-SBP) proposed in this work shows an high activity yield (of 21.55%), with a significant reduction of the material citotoxicity (cell damage and oxidative stress). The presence of SBP on the surface of the (SGAu-C-G-SBP) functionalized glass does not seem to influence the glass bioactivity and, in particular, the abundant presence on (SGAu-C-G-SBP) of brushite, formed during the functionalization steps, can be considered a favourable condition for HA/HCA crystallization, symptom of bioactivity.

What was obtained here, SBP immobilized onto sol-gel bioactive glasses exploiting SAMs formation, can be thus regarded as a novel bio-conjugate material, that is easy to use and allows to obtain stable and reproducible devices.

Acknowledgments. This research was financed with funds from the Italian Ministry MIUR (project PRIN2006, ‘‘Interface phenomena in silica-based nanostructured biocompatible materials contacted with biological systems” prot. 2006032335, Area 03). Authors from the University of Modena and Reggio Emilia thank the “Centro Interdipartimentale Grandi Strumenti” (CIGS) of the University of Modena e Reggio Emilia for instrument availability and assistance.

References

[1] Cao, W.; Hench, L.L. Bioactive Materials, *Ceram. Int.* **1996**, 22, 493-507.

[2] Gupta, R.; Kumar, A. Bioactive materials for biomedical applications using sol-gel technology, *Biomed. Mater.* **2008**, 3, 34005-34020.

[3] Abou-Neel, E.A.; Pickup, D.M.; Valappil, S.P.; Newport, R.J.; Knowles J.C. Bioactive functional materials: a perspective on phosphate-based glasses, *J. of Mat. Chem.* **2009**, 19, 690-701.

[4] Mansur, H.S.; Orefice, R.L.; Vasconcelos, W.L.; Lobato, Z.P.; Machado, L.J.C. Biomaterial with chemically engineered surface for protein immobilization, *J. of Mat. Sci.–Mat. in Med.* **2005**, 16, 333-340.

[5] Menaa, B.; Menaa, F.; Aiolfi-Guimaraes, C.; Sharts, O. Silica-based nanoporous sol-gel glasses: from bioencapsulation to protein folding studies, *Inter. J. of Nanotech.* **2010**, 7, 1-45.

[6] Colilla, M.; Izquierdo-Barba, I.; Vallet-Regi, M. Novel biomaterials for drug delivery, *Exp. Opin. on Therap. Patents* **2008**, 18, 639-656.

[7] Hench, L.L. Sol–gel materials for bioceramic applications, *Curr. Opin.. in Sol. State and Mat. Sci.* **1997**, 2, 604-610.

[8] Hanefeld, U.; Gardossi L.; Magner, E. Understanding enzyme immobilisation, *Chem. Soc. Rev.* **2009**, 38, 453-468.

[9] Kim, J.; Grate, J.W.; Wang, P. Nanostructures for enzyme stabilization, *Chem. Eng. Sci.* **2006**, 61, 1017-1024.

[10] Mahony, O.; Jones, J.R. Porous bioactive nanostructured scaffolds for bone regeneration: a sol-gel solution, *Nanomed.* **2008**, 3, 233-245.

[11] Kokubo T.; Takadama, H. How useful is SBF in predicting in vivo bone bioactivity? *Biomaterials* **2006**, 27, 2907-2915.

[12] Vallet-Regí, M.; Izquierdo-Barba, I.; Salinas, A.J. Influence of P2O5 on crystallinity of apatite formed in vitro on surface of bioactive glasses, *J. Biomed. Mater. Res.* **1999**, 46, 560-565.

[13] Weetall, H.H. Covalent coupling methods for inorganic support materials. *In Methods in Enzymology Klaus M. Ed. Academic Press* **1976,** 44, 134-148.

[14] Weetall, H.H. Enzymes immobilized on inorganic supports, *Trends in Biotech.* **1985**, 3, 276-280.

[15] Walt, D.R.; Agayn, V.I. The chemistry of enzyme and protein immobilization with glutaraldehyde, *Trends in Anal. Chem.* **1994**, 13, 425-430.

[16] D. Chen and J. Li, Interfacial design and functionization on metal electrodes through self-assembled monolayers, *Surf. Sci. Rep.* **2006**, 61, 445-463.

[17] Taylor-Pashow, K.M.L.; Della Rocca, J.; Huxford R.C.; Lin, W. Hybrid nanomaterials for biomedical applications, *Chem. Comm.* **2010**, 46, 5832-5849.

[18] Ghosh, P.; Han, G.; De, M.; Kim C.K.; Rotello M. Gold nanoparticles in delivery applications, *Adv. Drug Del. Rev.* **2008**, 60, 1307-1315.

[19] Boisselier, E.; Astruc, D. Gold nanoparticles in nanomedicine: preparations, imaging, diagnostics, therapies and toxicity, *Chem. Soc. Rev.* **2009**, 38, 1759-1782.

[20] Lusvardi, G.; Malavasi, G.; Aina, V.; Bertinetti, L.; Cerrato, G.; Magnacca, G.; Morterra C.; Menabue, L. Bioactive Glasses Containing Au Nanoparticles. Effect of Calcination Temperature on Structure, Morphology, and Surface Properties, *Langmuir* **2010,** 26, 10303-10314.

[21] Kinov, P.; Leithner, A.; Radl, R.; Bodo, K.; Khoschsorur, G.A.; Schauenstein, K.; Windhager, R. Role of free radicals in aseptic loosening of hip arthroplasty, *J. of Orthop. Res.* **2006**, 24, 55-62.

[22] Galecka, E.; Jacewicz R.; Mrowicka, M. Antioxidative enzymes--structure, properties, functions, *Pol. Merkur. Lekarski.* **2008**, 25, 266-268.

[23] Kucukakin, B.; Gogenur, I.; Reiter R.J.; Rosemberg, J. Oxidative Stress in Relation to Surgery: Is There a Role for the Antioxidant Melatonin? *J. of Surg. Res.* **2009**, 152, 338-347.

[24] O'Brien, P. Peroxidases, *Chem. Biol. Interact.*. **2000**, 129**,** 113-139.

[25] Floris, R.; Piersma, S.R.; Yang, G.; Jones P.; Wever, R. Interaction of myeloperoxidase with peroxynitrite *Eur. J. of Biochem.* **1993**, 215**,** 767-775.

[26] Grace, S.C.; Salgo, M.G.; Pryor, W.W. Scavenging of peroxynitrite by a phenolic/peroxidase system prevents oxidative damage to DNA, *FEBS Lett.* **1998,** 426**,** 24-28.

[27] Trujillo, M.; Ferrer-Sueta, G.; Radi, R. Peroxynitrite detoxification and its biologic implications. *Antioxidants & Redox Signaling* **2008**, 10, 1607-1619.

[28] Henriksen, A.; Mirza, O.; Indiani C.; Teilum, K.; Smulevich, G.; Welinder, K.; Gajhede, M. Structure of soybean seed coat peroxidase: A plant peroxidase with unusual stability and haem-apoprotein interactions. *Protein Sci.* **2001**, 10, 108-115.

[29] Kamal, J.K.A.; Behere, D.V. Thermal and Conformational Stability of Seed Coat Soybean Peroxidase. *Biochemistry* **2002**, 41**,** 9034-9042

[30] McEldoon, J.P.; Dordick, J.S. Unusual Thermal Stability of Soybean Peroxidase. *Biotechnol. Prog.* **1996**, 12**,** 555-558.

[31] Boscolo, B.; Laurenti, E.; Ghibaudi, E. ESR Spectroscopy Investigation of the Denaturation Process of Soybean Peroxidase Induced by Guanidine Hydrochloride, DMSO or Heat. *Prot. J.* **2006**, 25, 379-390.

[32] Verne´, E.; Vitale-Brovarone, C.; Bui, E.; Bianchi C.L.; Beccaccini, A.R. Surface functionalization of bioactive glasses, *J. Biomed. Mater. Res.* **2009**, 90A, 981-992.

[33] Verné, E.; Ferrarsi, S.; Vitale-Brovarone, C.; Spriano, S.; Bianchi, C.L.; Naldoni, A.; Morra M.; Cassinelli, C. Alkaline phosphatase grafting on bioactive glasses and glass ceramics, *Acta Biomaterialia* **2010**, 6, 229-240.

[34] Kamal, J.K.A.; Behere, D.V. Activity, stability and conformational flexibility of seed coat soybean peroxidase, *J. Inorg. Biochem.* **2003**, 94, 236-242.

[35] Ngo, T.T.; Lenhoff, H.M. A sensitive and versatile chromogenic assay for peroxidase and peroxidase coupled reactions *Anal. Biochem.* **1980**, 105, 389-397.

[36] Aina, V.; Perardi, A.; Bergandi, L.; Malavasi, G.; Manabue, L.; Morterra C.; Ghigo, D. Cytotoxicity of zinc-containing bioactive glasses in contact with human osteoblasts, *Chem. Biol. Interact.* **2007**, 167**,** 207-218.

[37] Gerard-Monnier, D.; Erdelmeier, I.; Regnare, K.; Moze-Henry, N.; Yadan J.C.; Chaudiere, J. Reactions of 1-methyl-2-phenylindole with malondialdehyde and 4-hydroxyalkenals. Analytical applications to a colorimetric assay of lipid peroxidation, *Chem. Res. Toxicol.* **1998**, 11, 1176-1183.

[38] Aina, V.; Marchis, T.; Laurenti, E.; Diana, E.; Lusvardi, G.; Malavasi, G.; Menabue, L.; Cerrato G.; Morterra, C. Functionalization of Sol Gel Bioactive Glasses Carrying Au Nanoparticles: selective Au Affinity for Amino and Thiol Ligand Groups, *Langmuir*, **2010**, 26(24), 18600-18605.

[39] Colthup L.H.; Wiberley, D.S.E. Introduction to infrared and Raman spectroscopy, *Academic Press, London*, **1975**.

[40] PCPFWIN Version 2.3; JCPDS (Joint Committee on Powder Diffraction Standards) International Center for Diffraction Data; Swarthmore, PA, **2002**.

[41] Kingery, W.D.; Bowen, H.K.;. Uhlmann, D.R Introduction to Ceramics. *2nd Ed. John Wiley&Son, Canada*, **1976**.

[42] Trpkovska, M.; Soptrajanov, B.; Malkov, P. FTIR reinvestigation of the spectra of synthetic brushite and its partially deuterated analogues, *J. Mol. Struct.* **1999**, 481, 661-666.

[43] Kumar, M.; Dasarathy, H.; Riley, C. Electrodeposition of brushite coatings and their transformation to hydroxyapatite in aqueous solutions, *J. Biomed. Mater. Res.* **1999**, 45, 302-310.

[44] Kumar, M.; Xie, J.; Chittur K.; Riley C. Transformation of modified brushite to hydroxyapatite in aqueous solution: effects of potassium substitution, *Biomaterials* **1999**, 20, 1389-1399.

[45] Lin, F.H.; Yao, C.H.; Sun, J.S.; Liu H.C.; Huang, C.W. Biological effects and cytotoxicity of the composite composed by tricalcium phosphate and glutaraldehyde cross-linked gelatine, *Biomaterials* **1998**, 19, 905-917.

[46] Gough, J.E.; Scotchford, C.A.; Downes, S. Cytotoxicity of glutaraldehyde crosslinked collagen/poly(vinyl alcohol) films is by the mechanism of apoptosis, *J. Biomed. Mater. Res.* **2002**, 61, 121–130.

[47] Scotchford, C.A.; Cascone, M.G.; Downes S.; Giusti, P. Osteoblast responses to collagen-PVA bioartiÞcial polymers in vitro: the effects of cross-linking method and collagen content, *Biomaterials* 1998, 19, 1-11.

[48] Huang-Lee, L.L.; Cheung D.T.; Nimni, M.E. Biochemical changes and cytotoxicity associated with the degradation of polymeric glutaraldehyde derived crosslinks, *J. Biomed. Mater. Res.* 1990, 24, 1185-201.

Figure Captions.

Fig. 1. SEM–EDS analysis of SGAu as such (A), SGAu-C (B), SGAu-C-G (C), and SGAu-C-G-SBP (D). EDS data report the composition, expressed as atomic %, as a mean of four measurements (std. dev. = 0.5%).

Fig. 2. Absorbance FTIR spectra, in the analytical spectral range 1800–400 cm^{-1}, of diluted KBr pellets. **Section A**: SGAu glass as such [spectrum (a)]; SGAu glass functionalized with cysteamine [spectrum (b)]; no-gold SG glass functionalized with cysteamine [spectrum (b')]; the reference spectrum of pure cysteamine [spectrum (1)]. **Section B**: cysteamine-functionalized SGAu glass [spectrum (a)]; SGAu glass functionalized with cysteamine + glutaraldehyde [spectrum (c)]; the reference spectrum of pure glutaraldehyde [spectrum (2)]. **Section C**: SGAu glass functionalized with cysteamine + glutaraldehyde [spectrum (c)]; SGAu glass functionalized with cysteamine + glutaraldehyde + SBP [spectrum (d)]; [spectrum (e)]; the reference spectrum of pure SBP [spectrum (3)].

Fig. 3. XRD patterns of the glass carrying AuNPs, isolated after the various steps of the functionalization process (as indicated by the sample symbols). In each section, two diffraction patterns are reported: one (black-line traces) is relative to the samples as-such (*i.e.*, after the relevant functionalization reaction step), and the other (red-line traces) to the same samples after 7 days of soaking in MEM solution. (Au: gold; HA: hydroxyapatite; g-SiO_2: silica gel; B: brushite).

Fig. 4. Absorbance FTIR spectra, in the analytical spectral range 1800–400 cm^{-1}, of diluted KBr pellets of as-such SGAu-glass in the four phases of the functionalization process [red-line spectra (a)], and after contact times with MEM solution of 1 hour [spectra (b)], 1 day [spectra (c)], and 7 days [spectra (d)]. **Section A:** the starting SGAu glass; **Section B:** SGAu glass functionalized with

cysteamine (SGAu-C); **Section C:** SGAu glass functionalized with cysteamine and glutaraldehyde (SGAu-C-G); **Section D:** SGAu glass functionalized with cysteamine, glutaraldehyde and SBP (SGAu-C-G-SBP).

Fig. 5. SEM–EDS analysis of the starting glass SGAu (A), SGAu-C (B), SGAu-C-G (C) and SGAu-C-G-SBP (D), isolated after 7 days of soaking in MEM solution. The reported EDS data express the composition as atoms %, and are the average of four measurements (std. dev. = 0.5%).

Fig. 6. Activity essay carried out on free SBP (□), SGAu-C-G-SBP (■), and SGAu-SBP Ads (▼). The enzymatic activities were calculated on the basis of the average initial rate of formation of the DMAB/MBTH reaction product, and are presented as micromolar concentration of product generated per minute (U) as function of enzyme concentration. Each test was carried out with $1.20 \cdot 10^{-3}$ M DMAB, $3.73 \cdot 10^{-5}$ M MBTH and $4.9 \cdot 10^{-5}$ M H_2O_2, varying the enzyme concentration between $1.25 \cdot 10^{-9}$ M and $2.00 \cdot 10^{-8}$ M.

Fig. 7. Comparison of catalytic activities of all the samples synthesized. The activities of SGAu as synthesized (SGAu), cysteamine functionalized SGAu (SGAu-C), glutaraldehyde-cysteamine functionalized SGAu (SGAu-C-G), immobilized SBP (SGAu-C-G-SBP), and adsorbed SBP (SGAu-SBP-Ads) were measured as the increase in absorbance at 590 min after 10 min of reaction time and related with the result obtained with free SBP taken as reference (100%). All the tests were carried out with $1.20 \cdot 10^{-3}$ M DMAB, $3.73 \cdot 10^{-5}$ M MBTH and $4.9 \cdot 10^{-5}$ M H_2O_2 at constant solid concentration (1.6 mg SGAu/ml).

Fig. 8. Effect of glass powders on LDH release in the supernatant of MG-63 cells. Cells were incubated in the absence (CTRL) or in the presence of cysteamine (Cyst) at the concentrations of 5, 10 and 20 nM that correspond to the amounts of cysteamine grafted onto 25, 50 and 100 μg of glass

respectively, glutaraldehyde (Glut) at the concentrations of 2.5, 5 and 10 nM that correspond to the amounts of glutaraldehyde grafted onto 25, 50 and 100 μg of glass respectively, soybean peroxidase (SBP) at the concentrations of 1, 2 and 4 pM that correspond to the amounts of SBP grafted onto 25, 50 and 100 μg of glass respectively, or of one of the following materials: AuNPs-containing bioactive glass (SGAu); cysteamine-functionalized glass (SGAu-C); glutaraldehyde-functionalized glass (SGAu-C-G); SBP-functionalized glass (SGAu-C-G-SBP); adsorbed SBP on the parent glass (SGAu-SBP-Ads) at three different concentrations 25, 50 and 100 μg/ml.

After a 24 hours incubation, the LDH activity was measured as described in Materials and Methods. Extracellular LDH activity was calculated as percentage of total (intracellular + extracellular) LDH activity in the dish. Measurements (n = 3) were performed in triplicate, and the data are presented as mean values ± SE. Vs CTRL * $p < 0.0001$.

Fig. 9. Effect of glass powders on intracellular MDA in MG-63 cells. Cells were incubated in the absence (CTRL) or presence of cysteamine (Cyst) at the concentrations of 5, 10 and 20 nM that correspond to the amounts of cysteamine grafted onto 25, 50 and 100 μg of glass respectively, glutaraldehyde (Glut) at the concentrations of 2.5, 5 and 10 nM that correspond to the amounts of glutaraldehyde grafted onto 25, 50 and 100 μg of glass respectively or soybean peroxidase (SBP) at the concentrations of 1, 2 and 4 pM that correspond to the amounts of SBP grafted onto 25, 50 and 100 μg of glass respectively or one of the following materials at three different concentrations 25, 50 and 100 μg/ml: AuNPs-containing bioactive glass (SGAu); cysteamine-functionalized glass (SGAu-C); glutaraldehyde-functionalized glass (SGAu-C-G); SBP-functionalized glass (SGAu-C-G-SBP); adsorbed SBP on glass (SGAu-SBP-Ads).

After 24 hours the intracellular MDA was measured as described in Materials and Methods.

Measurement (n = 3) were performed in triplicate, and data are presented as means ± SE. Vs CTRL * $p < 0.0001$.

Schemes

Scheme 1. Schematic representation of the different steps of glass functionalization

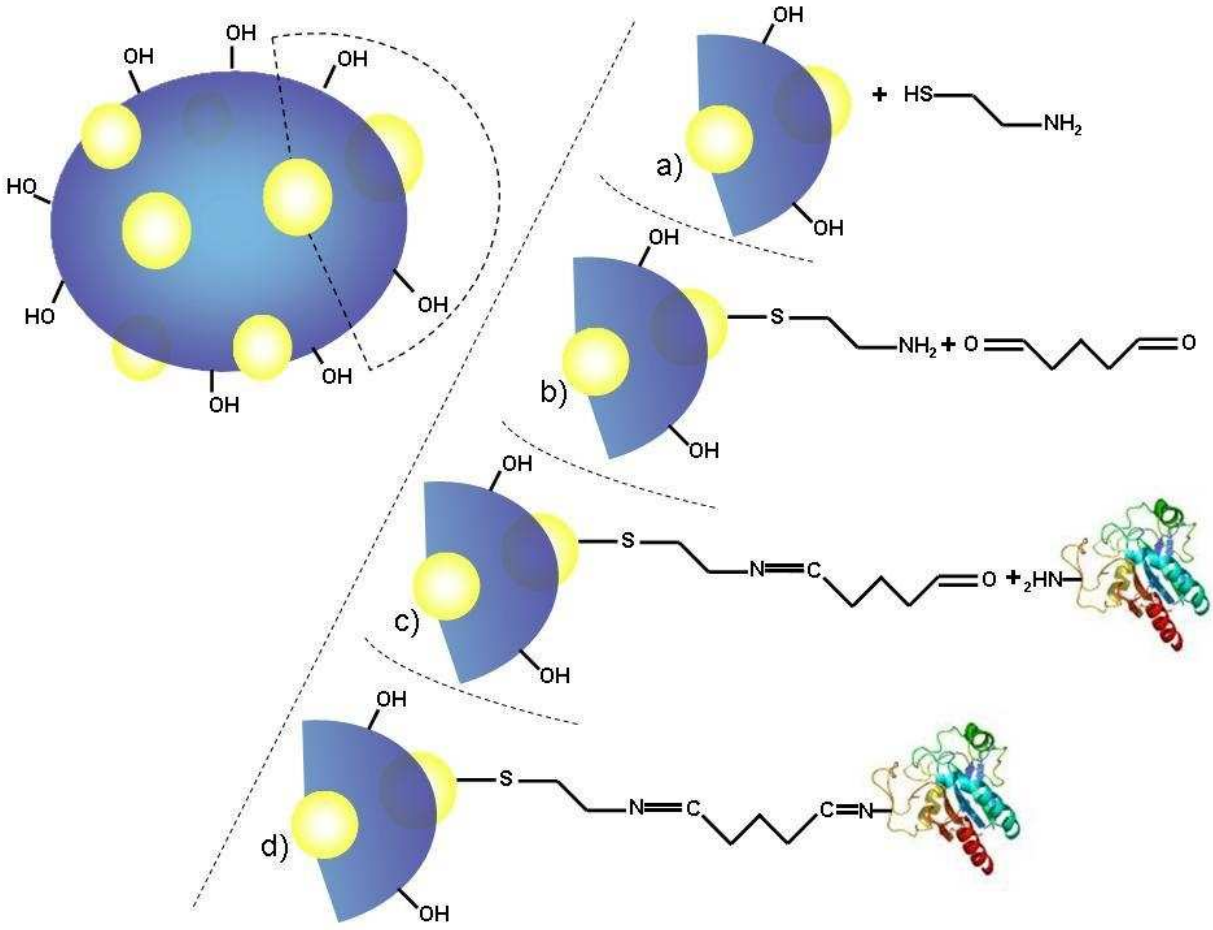

Tables

Table 1. Samples description, and abbreviations reported in the text.

Samples abbreviation	Samples description
SGAu	Bioactive glass containing gold nanoparticles, as such
SGAu-C	Bioactive glass containing gold nanoparticles functionalized with cysteamine
SGAu-C-G	Bioactive glass containing gold nanoparticles functionalized with cysteamine and glutaraldehyde
SGAu-C-G-SBP	Bioactive glass containing gold nanoparticles functionalized with cysteamine, glutaraldehyde and Soybean Peroxidases
SGAu-SBP-Ads	Soybean Peroxidases adsorbed on Bioactive glass containing gold nanoparticles

Table 2. Quantification of molecules present on the glass surface by the use of Elemental Analysis. Each value reported (± std.dev.) is the average of three analyses carried out on different samples.

Samples	%N	%C	%H	%S	mg/g_{glass}
SGAu	0.00	0.50±0.03	1.00±0.10	0.00	/
SGAu-C	0.25±0.02	0.95±0.05	1.30±0.12	0.50±0.10	13.8 of cysteamine
SGAu-C-G	0.23±0.02	1.27±0.05	1.37±0.11	0.45±0.08	13.8 of cysteamine + 10.0 of glutaraldehyde
SGAu-C-G-SBP	Not detectable				
SGAu-SBP-Ads	Not detactable				

Fig. 1. SEM–EDS analysis of SGAu as such (A), SGAu-C (B), SGAu-C-G (C), and SGAu-C-G-SBP (D). EDS data report the composition, expressed as atomic %, as a mean of four measurements (std. dev. = 0.5%).

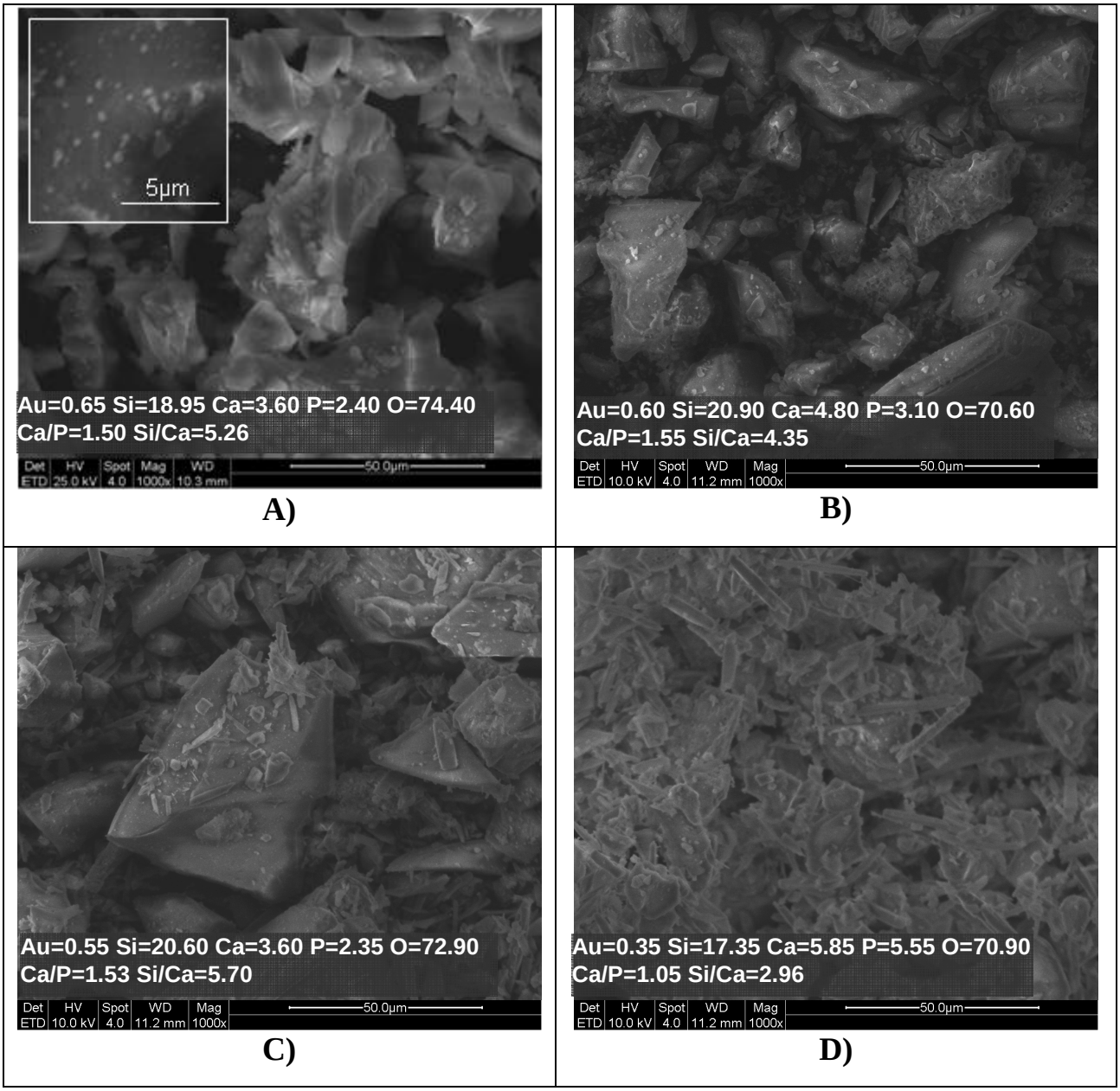

Fig. 2. Absorbance FTIR spectra, in the analytical spectral range 1800–400 cm^{-1}, of diluted KBr pellets. **Section A**: SGAu glass as such [spectrum (a)]; SGAu glass functionalized with cysteamine [spectrum (b)]; no-gold SG glass functionalized with cysteamine [spectrum (b')]; the reference spectrum of pure cysteamine [spectrum (1)]. **Section B**: cysteamine-functionalized SGAu glass [spectrum (a)]; SGAu glass functionalized with cysteamine + glutaraldehyde [spectrum (c)]; the reference spectrum of pure glutaraldehyde [spectrum (2)]. **Section C**: SGAu glass functionalized with cysteamine + glutaraldehyde [spectrum (c)]; SGAu glass functionalized with cysteamine + glutaraldehyde + SBP [spectrum (d)]; [spectrum (e)]; the reference spectrum of pure SBP [spectrum (3)].

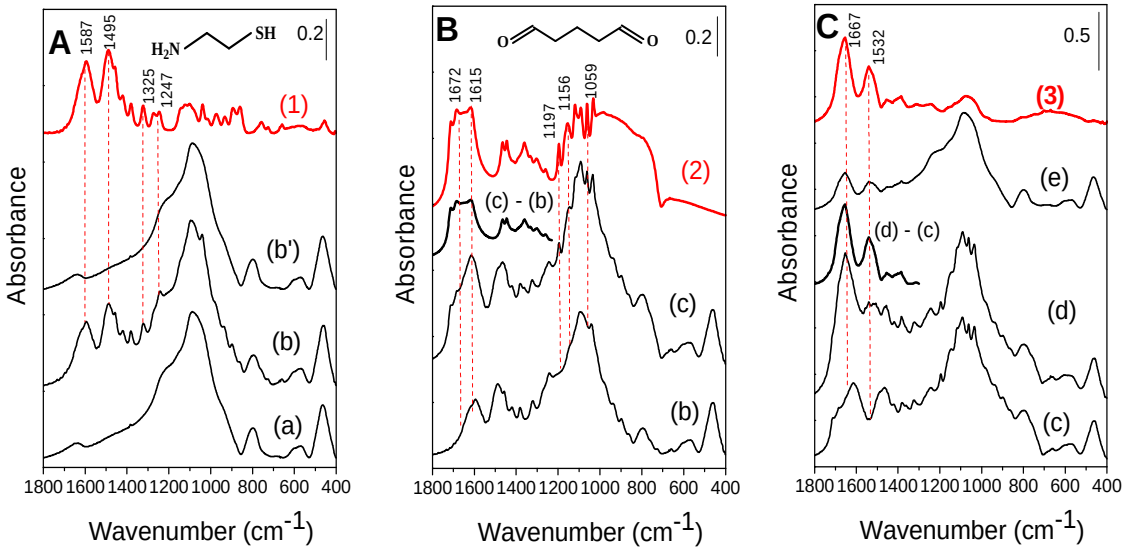

Fig. 3. XRD patterns of the glass carrying AuNPs, isolated after the various steps of the functionalization process (as indicated by the sample symbols). In each section, two diffraction patterns are reported: one (black-line traces) is relative to the samples as-such (*i.e.*, after the relevant functionalization reaction step), and the other (red-line traces) to the same samples after 7 days of soaking in MEM solution. (Au: gold; HA: hydroxyapatite; g-SiO_2: silica gel; B: brushite).

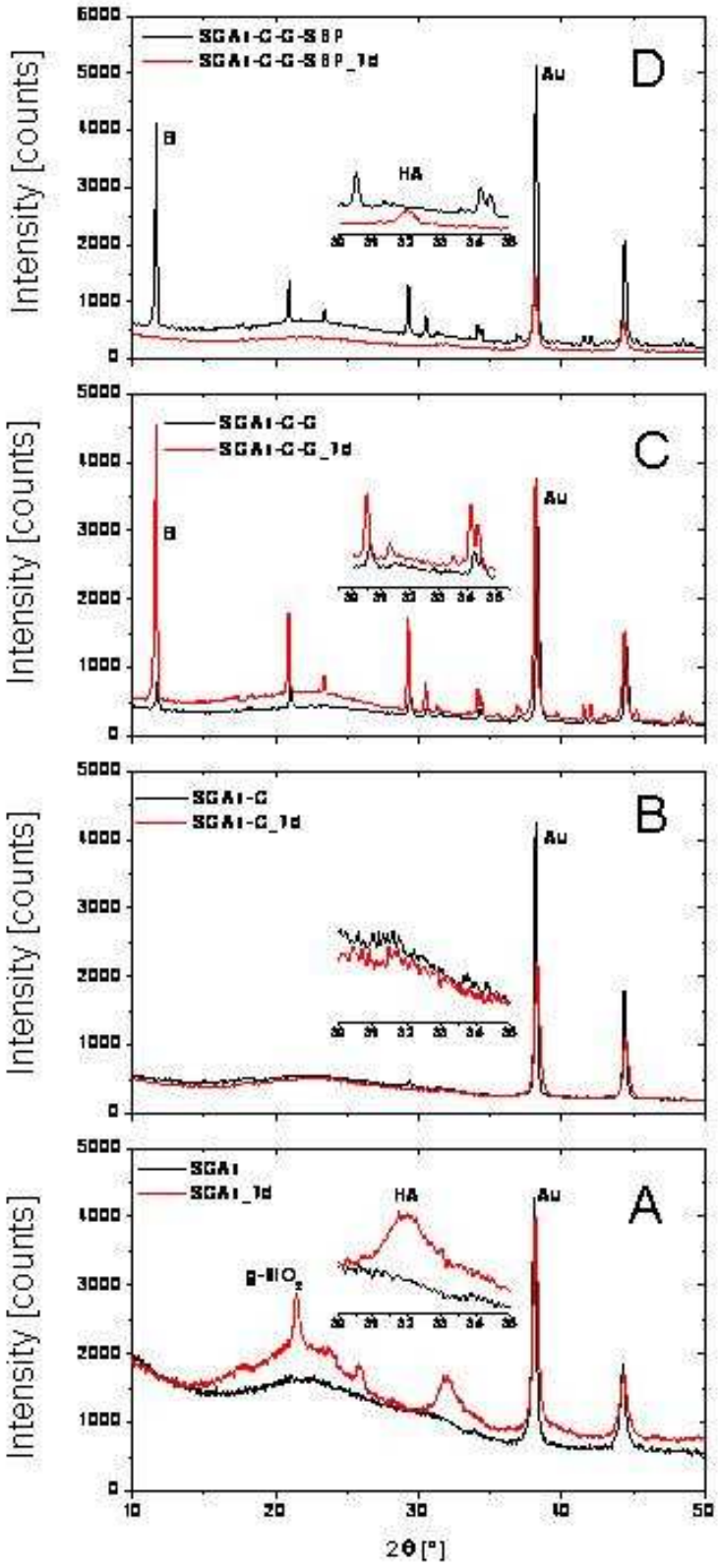

Fig. 4. Absorbance FTIR spectra, in the analytical spectral range 1800–400 cm^{-1}, of diluted KBr pellets of as-such SGAu-glass in the four phases of the functionalization process [red-line spectra (a)], and after contact times with MEM solution of 1 hour [spectra (b)], 1 day [spectra (c)], and 7 days [spectra (d)]. **Section A:** the starting SGAu glass; **Section B:** SGAu glass functionalized with cysteamine (SGAu-C); **Section C:** SGAu glass functionalized with cysteamine and glutaraldehyde (SGAu-C-G); **Section D:** SGAu glass functionalized with cysteamine, glutaraldehyde and SBP (SGAu-C-G-SBP).

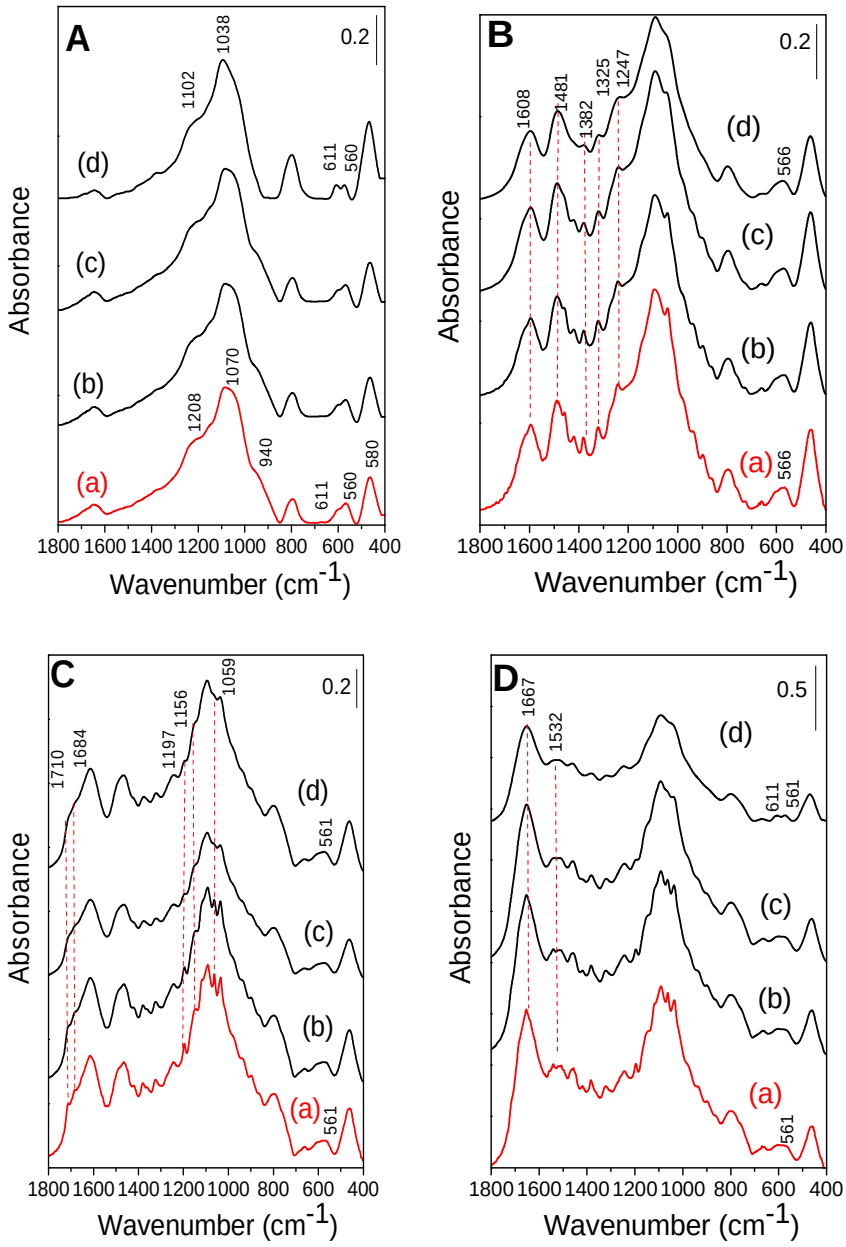

Fig. 5. SEM–EDS analysis of the starting glass SGAu (A), SGAu-C (B), SGAu-C-G (C) and SGAu-C-G-SBP (D), isolated after 7 days of soaking in MEM solution. The reported EDS data express the composition as atoms %, and are the average of four measurements (std. dev. = 0.5%).

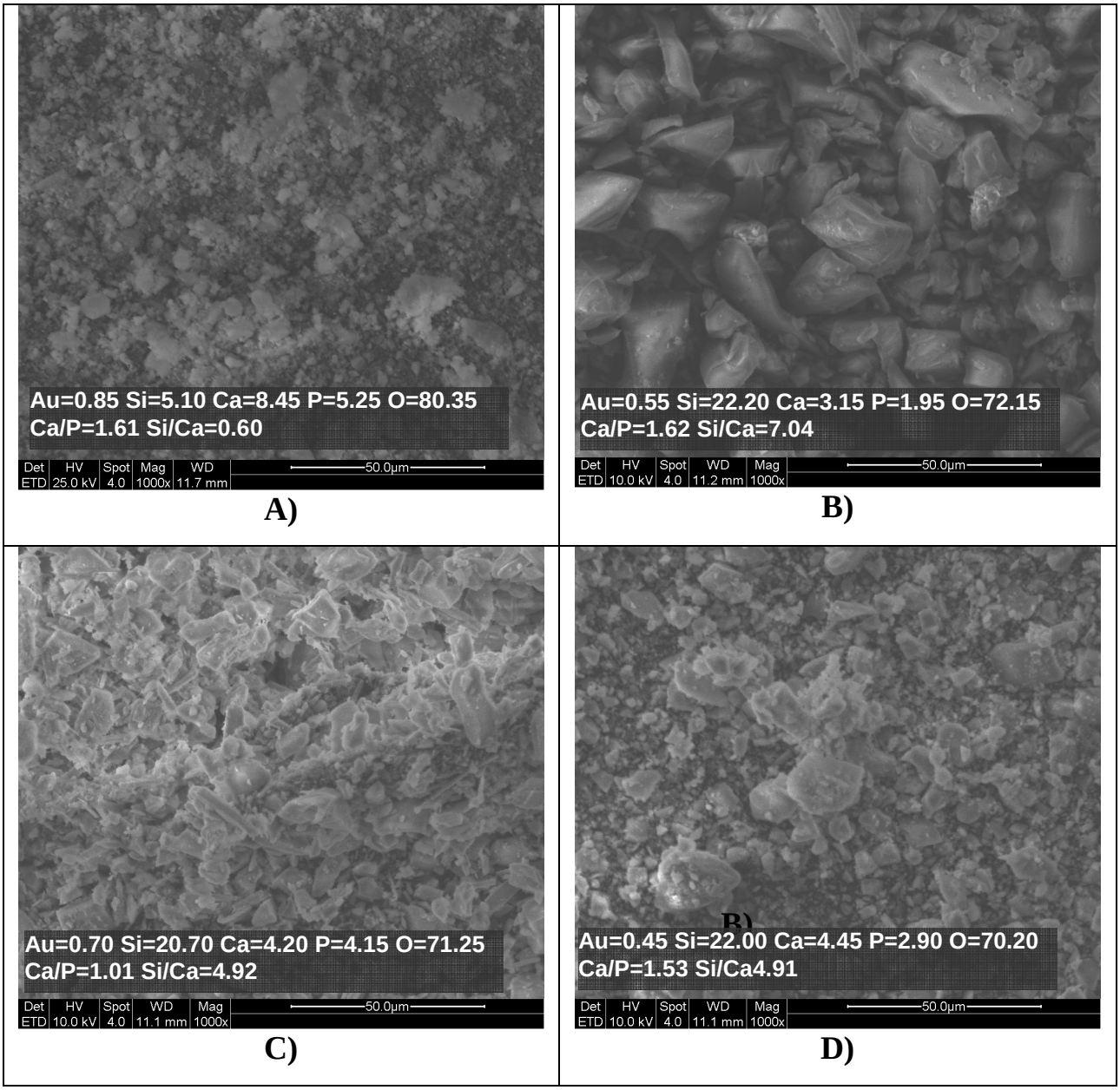

Fig. 6. Activity essay carried out on free SBP (□), SGAu-C-G-SBP (■), and SGAu-SBP Ads (▼). The enzymatic activities were calculated on the basis of the average initial rate of formation of the DMAB/MBTH reaction product, and are presented as micromolar concentration of product generated per minute (U) as function of enzyme concentration. Each test was carried out with $1.20 \cdot 10^{-3}$ M DMAB, $3.73 \cdot 10^{-5}$ M MBTH and $4.9 \cdot 10^{-5}$ M H_2O_2, varying the enzyme concentration between $1.25 \cdot 10^{-9}$ M and $2.00 \cdot 10^{-8}$ M.

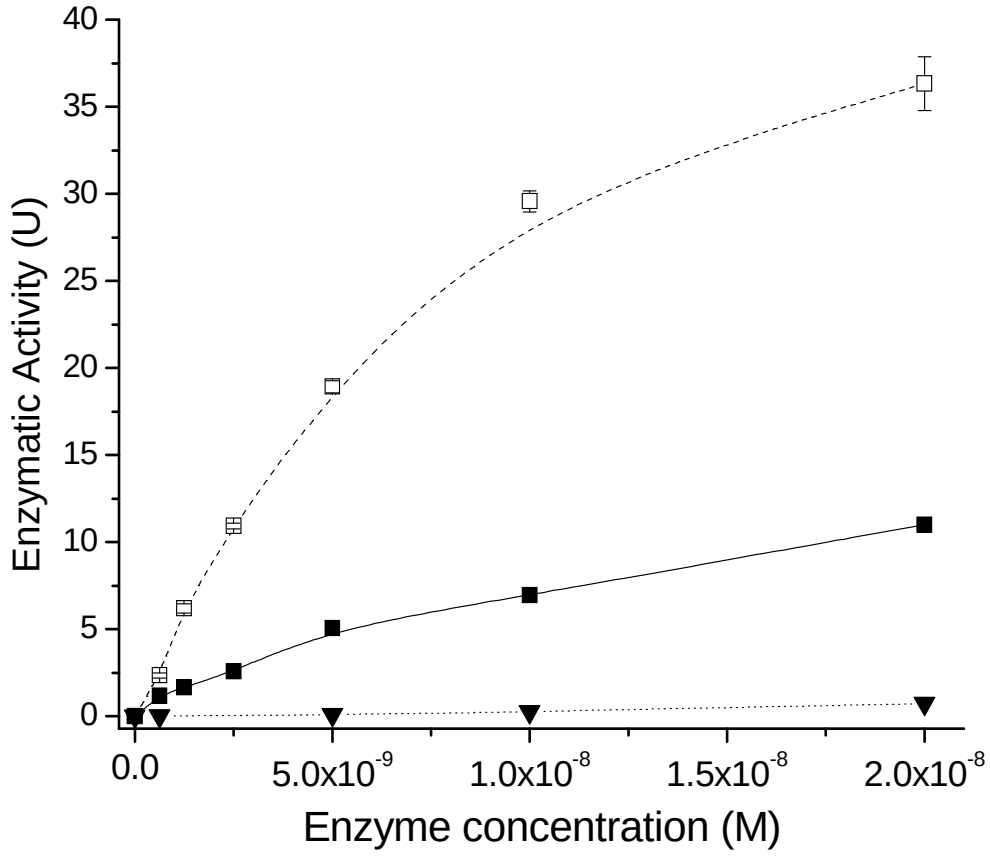

Fig. 7. Comparison of catalytic activities of all the samples synthesized. The activities of SGAu as synthesized (SGAu), cysteamine functionalized SGAu (SGAu-C), glutaraldehyde-cysteamine functionalized SGAu (SGAu-C-G), immobilized SBP (SGAu-C-G-SBP), and adsorbed SBP (SGAu-SBP-Ads) were measured as the increase in absorbance at 590 min after 10 min of reaction time and related with the result obtained with free SBP taken as reference (100%). All the tests were carried out with $1.20 \cdot 10^{-3}$ M DMAB, $3.73 \cdot 10^{-5}$ M MBTH and $4.9 \cdot 10^{-5}$ M H_2O_2 at constant solid concentration (1.6 mg SGAu/ml).

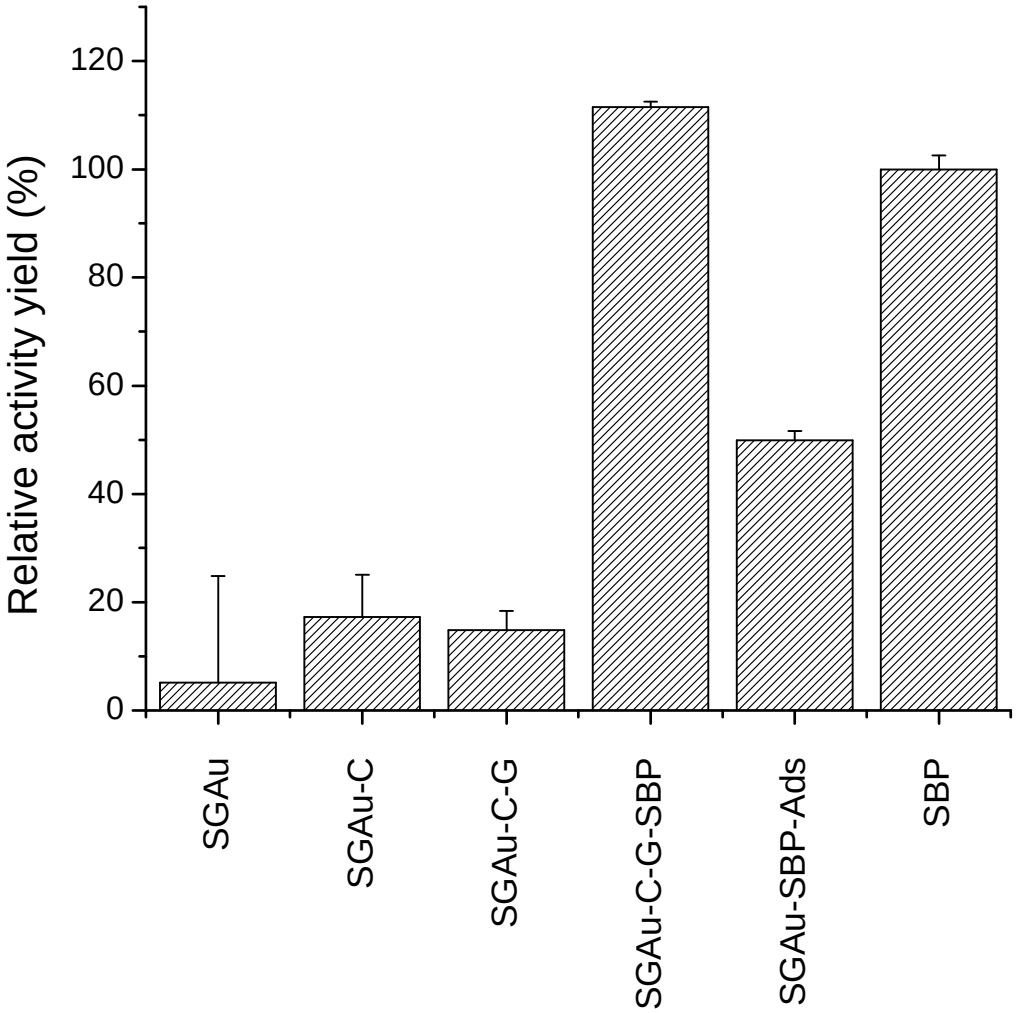

Fig. 8. Effect of glass powders on LDH release in the supernatant of MG-63 cells. Cells were incubated in the absence (CTRL) or in the presence of cysteamine (Cyst) at the concentrations of 5, 10 and 20 nM that correspond to the amounts of cysteamine grafted onto 25, 50 and 100 μg of glass respectively, glutaraldehyde (Glut) at the concentrations of 2.5, 5 and 10 nM that correspond to the amounts of glutaraldehyde grafted onto 25, 50 and 100 μg of glass respectively, soybean peroxidase (SBP) at the concentrations of 1, 2 and 4 pM that correspond to the amounts of SBP grafted onto 25, 50 and 100 μg of glass respectively, or of one of the following materials: AuNPs-containing bioactive glass (SGAu); cysteamine-functionalized glass (SGAu-C); glutaraldehyde-functionalized glass (SGAu-C-G); SBP-functionalized glass (SGAu-C-G-SBP); adsorbed SBP on the parent glass (SGAu-SBP-Ads) at three different concentrations 25, 50 and 100 μg/ml.
After a 24 hours incubation, the LDH activity was measured as described in Materials and Methods. Extracellular LDH activity was calculated as percentage of total (intracellular + extracellular) LDH activity in the dish. Measurements (n = 3) were performed in triplicate, and the data are presented as mean values ± SE. Vs CTRL * $p < 0.0001$.

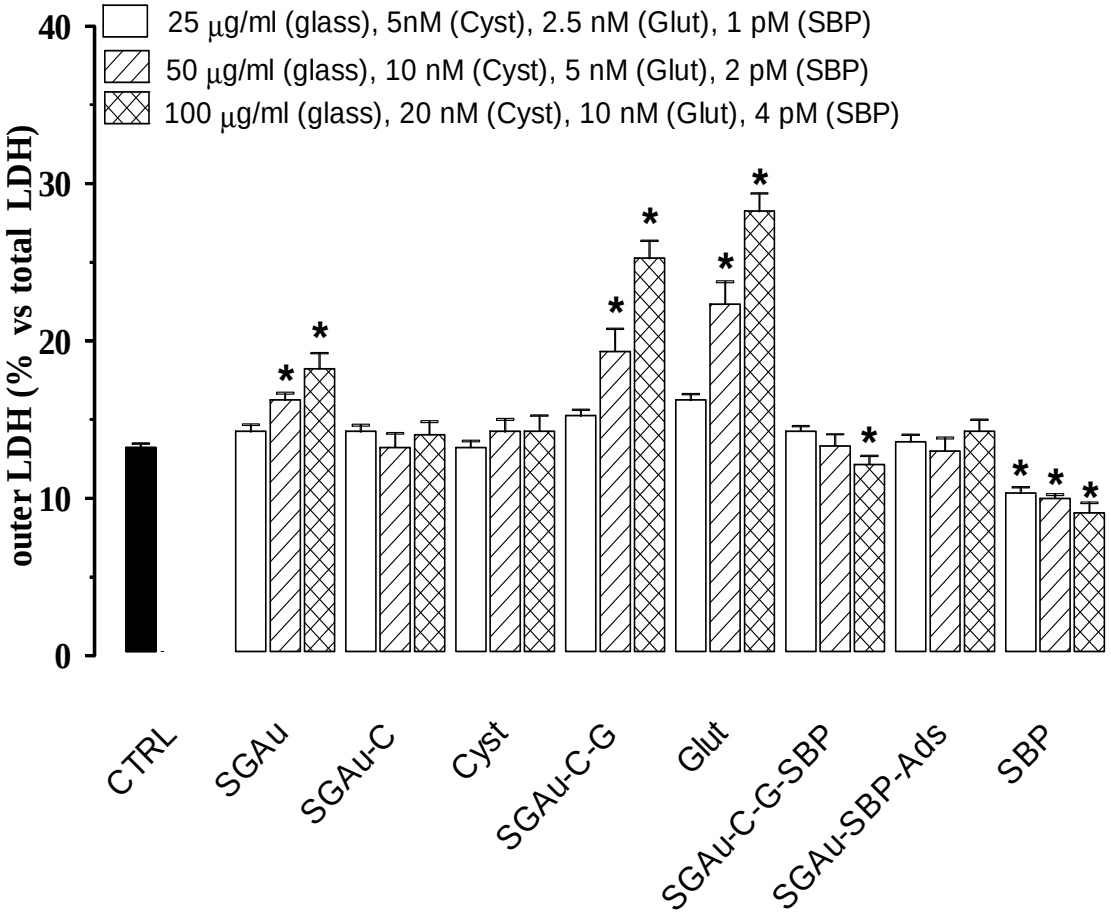

Fig. 9. Effect of glass powders on intracellular MDA in MG-63 cells. Cells were incubated in the absence (CTRL) or presence of cysteamine (Cyst) at the concentrations of 5, 10 and 20 nM that correspond to the amounts of cysteamine grafted onto 25, 50 and 100 μg of glass respectively, glutaraldehyde (Glut) at the concentrations of 2.5, 5 and 10 nM that correspond to the amounts of glutaraldehyde grafted onto 25, 50 and 100 μg of glass respectively or soybean peroxidase (SBP) at the concentrations of 1, 2 and 4 pM that correspond to the amounts of SBP grafted onto 25, 50 and 100 μg of glass respectively or one of the following materials at three different concentrations 25, 50 and 100 μg/ml: AuNPs-containing bioactive glass (SGAu); cysteamine-functionalized glass (SGAu-C); glutaraldehyde-functionalized glass (SGAu-C-G); SBP-functionalized glass (SGAu-C-G-SBP); adsorbed SBP on glass (SGAu-SBP-Ads).
After 24 hours the intracellular MDA was measured as described in Materials and Methods. Measurement (n = 3) were performed in triplicate, and data are presented as means ± SE. Vs CTRL * $p < 0.0001$.